Manuscript of the article: *Laszlo Banyai, Abdel-Monem Sayed Mohamed, Eszter Szűcs, Nadia Aboaly, Ashraf Mousa, Hassan Ahmed Khalil. The relationship between global plate motion and intra-plate deformation analysis of Cairo network: Case study with simulated data*, is copyrighted and appeared in: Arabian Journal of Geosciences, 2015, 9(1), 1-10

ISSN: 1866-7511 (Print) 1866-7538 (Online), Impact Factor: 1.224

doi: 10.1007/s12517-015-2096-9

The article is available electronically:

http://link.springer.com/article/10.1007/s12517-015-2096-9

The relationship between global plate motion and intra-plate deformation analysis of Cairo network: Case study with simulated data

Laszlo Banyai*, Abdel-Monem Sayed Mohamed**, Eszter Szűcs*, Nadia Aboaly**, Ashraf Mousa**, Hassan Ahmed Khalil**

*Research Centre for Astronomy and Earth Sciences, Sopron, Hungary

**National Research Institute of Astronomy and Geophysics, Helwan, Egypt

Keywords: plate motion, intra-plate deformation, GPS network, deformation analysis, seismicity, seismo-tectonics

Abstract. Although the Cairo region is classified as low and moderate seismological area, the frequent earthquakes (M=2-4) and the largest one at 12th October 1992 (M=5.9) prove the recent seismotectonic activity of the area, which is connected to the known fault systems. To monitor the tectonic changes GPS network was established in Cairo region and analyzed between 1986 and 2003. Because of technical reason the network was updated in 2011 and the data processing methods were reconsidered. The application of usual methods require a very careful approach since the Cairo Network is very fare from the known fiducial GPS stations at the African plate, the nearer fiducial stations are at different plates and the network is near to the plate borders. For the investigation of these circumstances UNAVCO plate motion calculator was used to simulate coordinate changes, and the impact of the chosen plate motion on the result of intra-plate deformations monitoring were analyzed. New data processing approach and integrated baseline adjustment and similarity transformation method is proposed as an alternative strategy for the regional size Cairo Network to estimate intra-plate deformations using GPS observations. The proposed method is demonstrated to estimate coordinate changes, global rotations and scale parameters in one computational step. The proposed method is used to investigate the significance of the impact of global plate motions on regional crustal movement network. Simulated data of the regional Cairo network is used for this evaluation. The estimated plate motions, simulated scale bias (due to miss-modeling of troposphere effect on GPS data) and baseline noise proved that the impact of plate motions have to be taken into account in the case of Cairo network if the investigation period is near or larger than ten years.

Introduction

Egypt is located in the northeastern part of Africa and extends beyond the Gulf of Suez and the Suez Canal into Asia. The tectonic evolution of Egypt is characterized by a number of stages since Precambrian. According to Said (1962); Youssef (1986) and Smith (1984), Egypt is classified into three major geological provinces (stable shelf, unstable shelf and Nubian Shield). The greater part of northern Egypt belongs to the unstable shelf which lies between foreland and geosyncline. Most of the area was covered by the principal marine transgressions at least since Paleozoic time. The main types of macrostructures in the study area are monoclines and faults. Moustafa et al. (1985) concluded that, the main structural features controlling the study area are the faults. Most of these faults have a Post Eocene age of deformation. The major faults that affect the study area have the NW-SE, E-W and NE-SW directions (Figure 1). The NW-SE trending faults are the most predominant ones. Analysis of these faults indicates that the main stress regime is the tensile stress (Abd El Tawab 1986). These tensile stresses are created from right lateral divergent strike slip movement on a deep seated of faults. All focal mechanism solutions in the Cairo region showed a normal faulting mechanism with a strike-slip component. Seismotectonic map of Cairo region is presented in Figure 1, where the known faults and the distribution of earthquakes epicenters between 1997 and 2012 with the magnitude larger than 2 are given.

Recent crustal movement monitoring was carried out in Cairo region after the earthquake in 12th October 1992 in Dahshour area, 35 km southwest Cairo City center with a magnitude of 5.9. This earthquake was felt over the whole area of Egypt. It caused a widespread damage in Cairo, Giza and El-Faiyum provinces. According to official reports about 8500 dwellings were destroyed, 561 people were killed, 6500 people were injured and the estimated damage is more than 35 million US dollar (Khater 1992; Thenhaus et al. 1993; Youssef et al. 1992).

GPS network was established in 1995 covering Cairo City and the southern part of the Nile Delta. It was selected according to the geological and geophysical considerations taking into account the requirements of GPS technique. The river Nile runs from south to north in the middle of the network. The initial measurements were carried out in 1996. The measurements were repeated once a year until 2007. Abdel-Monem (2005) presented and analyzed the data during the period from 1986 to 2003. Some points of the network were destructed, therefore the network was updated in 2011 and the initial measurements were performed in January 2012 (Abdel-Monem 2011). The names and numbers of the GPS stations are also included in Figure 1.

In this study simulated data are used to investigate the impact of global plate motions on the regional size Cairo network using GPS observation technique. Even in the case of small regional investigations, where we are interested only in the intra-plate changes of the network, it is reasonable to connect the network to the nearest permanent International Global Navigation Satellite System Service (IGS) fiducial station(s). Taking into account the actual coordinates of the IGS station(s) the consonance with the precise ephemerides is warranted, but the global plate motions of the regional network is also inherited.

It may be disadvantageous if the IGS station(s) are very far from the regional network, they are at different tectonic plates or the network is near to the plate borders. In the case of Cairo Network all the three circumstances have to be taken into account. The global motions of the networks determined in different observational epoch are usually subtracted by seven parameter similarity transformations (sometimes combined with estimated plate motions) and the residuals are investigated for intra-plate deformations.

In the case of Cairo network the following measurement and alternative data processing approach may be also reasonable:

1- Initial epoch:

1. adjustment of raw GPS observations together with nearest IGS station(s) and precise ephemerides (using e.g. Bernese software, the resulted coordinates are treated as preliminary coordinates)
2. independent adjustment of properly selected redundant baselines of GPS network without IGS station(s) (using e.g. Bernese software and coordinates from step 1)
3. network adjustment of baselines (from step 2) so that the squares sum of the coordinate changes (with respect to step 1) is minimized (these will be the reference coordinates of the investigations)

2- i-th epoch:

1. the same as initial epoch step1.
2. the same as initial epoch step2.
3. network adjustment of baselines (from step 2) so that the squares sum of the coordinate changes (with respect to step 3 of initial epoch) is minimized, if it is necessary global rotations and scale parameter can be estimated simultaneously.

The proposed method is tested using simulated data of Cairo network. The result of the proposed technique is compared with the traditional analysis techniques using the linearized seven parameter similarity transformation. The proposed method is suitable and efficient for estimating intra-plate motions of such regional networks. The effect of global plate tectonics is significant in the case of Cairo network and must be handled by care when producing intra-plate deformations.

1. Methodology and test computations

The sketch of the Cairo Network and the properly selected redundant baselines are presented in Figure 2. Those baselines that are longer than the line 200-600 are not selected. The baseline lengths are between 22 and 69 kilometers.

The coordinates of the *initial epoch* and their estimated changes providing the *i-th epoch* coordinates are given in Table 1. The coordinate changes for ten years period are computed by the UNAVCO plate motion calculator using the "ITRF2000D&A" model (Drewes and Angermann 2001), which estimates the coordinate changes in three Cartesian components (web of UNAVCO plate motion calculator, 2012). Figure 3 shows the horizontal changes of the network due to the plate motion simulation for ten years. The north components have a mean and standard deviation: 0.1697 ±0.0006 m, the east components have 0.2455 ±0.0005 m respectively, moreover no height changes are simulated by the used model.

To convert the three components of the plate motions into the rotations about the coordinate axes the well-known linearized seven parameter similarity transformation is applied (Spath 2004):

$$\begin{bmatrix} X \\ Y \\ Z \end{bmatrix}_{II} = \begin{bmatrix} X \\ Y \\ Z \end{bmatrix}_{I} + \begin{bmatrix} 1 & 0 & 0 & 0 & -Z & Y & X \\ 0 & 1 & 0 & Z & 0 & -X & Y \\ 0 & 0 & 1 & -Y & X & 0 & Z \end{bmatrix}_{I} \begin{bmatrix} t_x \\ t_y \\ t_z \\ R_x \\ R_y \\ R_z \\ sc \end{bmatrix} \quad (1)$$

where t_x, t_y, t_z are the translations, R_x, R_y, R_z are the rotations and *sc* is a scale parameter (the difference from unity). The subscripts *I* and *II* distinguish the two coordinate systems. In the case of equation (1) the system *I* is shifted, rotated and scaled to fit into system *II*.

The least-squares adjustment of the observational equations (1) can be used to estimate the seven parameters in the global coordinate system. If the coordinates are shifted to the center of gravity the alternative solution can be computed directly as:

$$dx = X_{II} - X_I\,, \qquad dy = Y_{II} - Y_I\,, \qquad dz = Z_{II} - Z_I\,,$$

$$t_x = \frac{\sum dx}{n}\,, \qquad t_y = \frac{\sum dy}{n}\,, \qquad t_z = \frac{\sum dz}{n}\,,$$

$$R_x = \frac{\sum(Z_{Ic}d_y - Y_{Ic}d_z)}{\sum(Z_{Ic}^2 + Y_{Ic}^2)}\,, \quad R_y = \frac{\sum(-Z_{Ic}d_x + X_{Ic}d_z)}{\sum(Z_{Ic}^2 + X_{Ic}^2)}\,, \quad R_z = \frac{\sum(Y_{Ic}d_x - X_{Ic}d_y)}{\sum(Y_{Ic}^2 + X_{Ic}^2)}\,, \quad (2)$$

$$sc = \frac{\sum(X_{Ic}d_x + Y_{Ic}d_y + Z_{Ic}d_z)}{\sum(X_{Ic}^2 + Y_{Ic}^2 + Z_{Ic}^2)}\,,$$

where n is a number of included stations and the subscript *Ic* refer to the coordinates in shifted system. In the case of the presented transformations the input coordinates are treated by using equal unit weights.

For the new method, the effects of the transformation on the GPS derived baseline components for stations *i* and *j* can be modeled using equation (1) as:

$$\begin{bmatrix} \Delta X_{ij} \\ \Delta Y_{ij} \\ \Delta Z_{ij} \end{bmatrix}_{II} = \quad (3)$$

$$\begin{bmatrix} 1 & 0 & 0 & -1 & 0 & 0 & 0 & -(Z_i - Z_j) & (Y_i - Y_j) & (X_i - X_j) \\ 0 & 1 & 0 & 0 & -1 & 0 & (Z_i - Z_j) & 0 & -(X_i - X_j) & (Y_i - Y_j) \\ 0 & 0 & 1 & 0 & 0 & -1 & -(Y_i - Y_j) & (X_i - X_j) & 0 & (Z_i - Z_j) \end{bmatrix}_{I} \begin{bmatrix} dx_i \\ dy_i \\ dz_i \\ dx_j \\ dy_j \\ dz_j \\ R_x \\ R_y \\ R_z \\ sc \end{bmatrix},$$

where the right hand side is composed of the initial coordinates and dx, dy, dz are the unknown coordinate changes.

The system of equations (3) can be used as the extended observation equations of the least-square adjustment including global rotations and scale parameter. In this case the equations contain three translational defects, three rotational defects and one scale defect. The singularities can be handled according to equation (2) by seven constraint equations:

$$\begin{gathered} \sum d_x = 0\,, \qquad \sum d_y = 0\,, \qquad \sum d_z = 0\,, \\ \sum(Z_{Ic}d_y - Y_{Ic}d_z) = 0\,, \quad \sum(-Z_{Ic}d_x + X_{Ic}d_z) = 0\,, \quad \sum(Y_{Ic}d_x - X_{Ic}d_y) = 0\,, \\ \sum(X_{Ic}d_x + Y_{Ic}d_y + Z_{Ic}d_z) = 0\,, \end{gathered} \tag{4}$$

which force no global translations, no rotations and no scale bias with respects to the initial coordinates, these effects are absorbed by the additional global unknowns as a results of the above constraints. The resulted coordinate changes describe only the intra-plate deformations of the network. This method is the combined baseline adjustment and similarity transformation in one integrated adjustment step. If no rotations and no scale are estimated only the translational constraints have to be used (first row of Eq. 4), which is equivalent to the free network approach of the baseline adjustment. The extended model and the seven constraints provide also free-network solution (Mierlo 1980), where the squares sum of coordinate changes is minimized. This procedure was implemented in the baseline adjustment software developed for different purposes (Banyai 1991, 2005).

During the test computations the baseline components are treated as uncorrelated quantities with 1 mm a priori standard deviations. In that case they can be compared to the results of similarity transformations.

2. Results and discussion

It is evident that the translations and the scale bias should be zero in the case of global similarity transformation. The very small discrepancies are the consequences of the truncations of the plate motion calculator after the fourth decimal digit. In the case of shifted transformation the estimated translations are the same as the mean values computed in Table 1. The rotations are the same in both cases. The results of the global and the shifted transformations of the initial epoch (*I*) and the simulated epoch (*II*) are given in Table 2.

The changes of the selected baselines (Figure 2) with respect to the initial values are given in Table 3. The mean changes are practically zeroes, but their standard deviations are very similar to the relevant values in Table 1. It shows that the residual plate motions are only few millimeters. To estimate the impact of these residuals, the baselines were adjusted using only translational constraints. The coordinate changes are summarized in Table 4. It is very interesting that the residual plate motions are absorbed mainly by the vertical components (Figure 4), which shows the tilt of the network in the direction of the global motions.

The similarity transformation was repeated using the newly adjusted coordinates, where the mean effect of plate motion had already been cancelled by the network adjustment. The surprising result can be found in Table 5. The network preserved the translational and rotational features of the plate motions. In the global model the translations are preserved in millimeter level, but with different signs

During the adjustment of raw GPS observations the not properly modeled atmospheric effects may cause a scale bias, as well. To study the effects of small 0.05 ppm scale bias a new data set was simulated (Table 6). The magnitude of the standard deviations is similar to the plate

motion residuals. The change of the baselines reflects only scale bias. The results of the baseline adjustment using only translational constraints are given in Table 7.

Contrary to the plate motions the vertical changes are zeroes. The horizontal changes are shown in Figure 5. The transformation of the new coordinates is given in Table 8. Both transformations preserved the zero rotations and the simulated scale bias. However the translations of the global solution compensate only the fact that the global coordinates are scaled, which shift the stations further from the global center.

The baselines composed from the sum of plate motion and the additional scale bias was also adjusted at the same way as before. The results are summarized in Tables 9 and 10. It is not surprising that the sum of Tables 4 and 7 is very similar to Table 9. Therefore the Figures 4 and 5 are valid in this case, too. Both transformations are provided the same rotations and scales, but the translations are the combinations of rotation and scale effects. The discrepancies are a little bit worse because of the additional numerical truncations of the scale effects.

In the previous investigations only the numerical truncations were the only error sources of the simulated baselines. In the next investigations normally distributed residuals ($N(0,1)$ mm) were added to the baseline components. Consequently they contain plate motions, scale bias and white noise as well. The baseline residuals are given in Table 11.

The baselines were adjusted using only translational constraints. The coordinate changes and the transformations are summarized in Tables 12 and 13. The difference between Tables 13 and 10 shows the effect of the simulated random noise.

The adjustment was repeated by the combined baseline adjustment and similarity transformation (equations 3 and 4). The results can be found in Table 14. Comparing Tables 13 and 14, it can be concluded that the combined adjustment provided the same parameters.

In the next investigation the plate motions of stations 400, 500 and 600 were reduced by 10 percent to simulate single station intra-plate movements. During the combined adjustment these stations were not included in the derivation of the constraint equations (4). It means that the network is rotated about a new center. All the baselines are rotated and scaled, but the neglected stations are allowed to change freely (not involved in the minimum norm). The results are given in Table 15. The small changes with respect to Table 14 prove that the rotations, scale and single station movements were properly preserved, in spite of the fact that the large number of baseline connected to the three stations were not involved in the estimation of global parameters.

3. Summary and Conclusions

According to the geographic settings and the lack of near IGS stations an alternative procedure was demonstrated for the Cairo network to determine intra-plate changes together with the effect of global plate motions. This procedure involves the baseline adjustment and similarity transformation in one integrated computational step.

Simulated global plate motions, additional scale bias (0.05 ppm) and random errors ($N(0,1)$ mm) of the baseline components were used in the test computations. The global plate motions were converted to global rotations about the Cartesian coordinate axes.

Estimating 10 years plate motion (UNAVCO calculator, ITRF2000 D&A 2001 model) the selected GPS baseline components (22-69 km) contain only a few mm plate motion residuals. The usual adjustment of the baseline components (using only translational constraints)

provided only mm level changes mainly in the vertical components. However the similarity transformation proved that these small changes preserved the characteristics of the global plate motions as well.

The baseline residuals of the simulated scale bias are also in a few mm level. Contrary to the plate motion the network adjustment provided only small horizontal coordinate changes.

In spite of that, the simulated random errors are comparable to the residual plate motions and scale biases, the adjusted network preserved the simulated global effects. These global effects can be handled very efficiently using the presented integrated adjustment model.

In the case of significantly smaller time periods or in the case of significantly smaller networks the baseline residuals caused by global plate motions may be significantly smaller than the noise level of the estimated baselines. In that case there is no need for additional parameters; however, if the similarity transformations or the combined adjustments indicate significant biases, the sources of these biases have to be found in the adjustment procedure or in the quality of the raw GPS observations.

In the case of Cairo Network it is reasonable to estimate the impact of the global plate motions during longer investigational periods. The proposed strategy and the integrated adjustment should be tested using real observations as one of the possible options.

Acknowledgement This study was carried out under the scientific cooperation agreement between the National Research Institute of Astronomy and Geophysics, Helwan, Egypt and the Research Centre for Astronomy and Earth Sciences, Sopron, Hungary.

References

Abdel-Monem SM (2005) Using compiled seismic and GPS data for hazard estimation in Egypt. NRIAG, Journal of Geophysics, Vol.4, No. 1, pp. 51-79.

Abdel-Monem SM (2011) Collaborative Research Project between Egyptian and Hungariann Acadimes (2012-2014) under the title Recent geodynamic investigations using geodetic methods.

Abd El Tawab S (1986) Structural Analysis of the Area Around Gebel El Mokattam, M.sc. Thesis, Geol. Dep. Fac. Sci., Ain Shams Univ., pp121.

Bányai L (1991) Treatment of rotation errors in the final adjustment of GPS baseline components. Bull. Geod. 65 , pp 102- 108.

Bányai L (2005) Investigation of GPS antenna mean phase centre offsets using a full roving observation strategy. Journal of Geodesy 79, pp. 222- 230.

Drewes H, Angermann D (2001) The Actual Plate Kinematic and Crustal Deformation Model 2000 (APKIM2000) as a Geodetic Reference System, AIG 2001 Scientific Assembly, Budapest, 2-8 Sept 2001.

Khater M (1992) Reconnaissance Reporton the Cairo, EgyptEarthquake of October 12, 1992. TechnicalRept. NCEER-92-0033, SUNY-Buffalo, Buffalo, NY, December.

Mierlo J van (1980) Free network adjustment and S-transformations. DGK Reiche B, 252.

Moustafa AR, Yehia MA, Abdel Tawab S (1985): Structural Setting of the Area East of Cairo, Maadi and Helwan, Mid. East. Res. Cont. Ain Shams Univ. Vol., 5, 40-64.

Said R (1962) The geology of Egypt, Elsevier publishing Company. Amsterdam / New York.

Smith CM. (1984) Geology of Egypt Rep. Schlumberger Oil Company, Well Evalution Conf. Cairo, Egypt.

Spath H (2004) A numerical method for determining the spatial HELMERT transformation in the case of different scale factors, Zeitschrift fur Vermessungswesen 129, pp. 255-259.

Thenhaus PC, Sharp RV, Celebi M, Ibrahim ABK, Van H (1993) Reconnaissance Report on the 12 October 1992 Dahshur, Egypt. Earthquake. U.S. GeologicalSurvey, Open-FileReport 93-181, Golden, CO.

UNAVCO plate motion calculator: http://www.unavco.org/community_science/science-support/crustal_motion/dxdt/model.html, Last visited June, 2015.

Youssef NS (1986) The regional structure map of Egypt. The American Association of Petroleum Gelogists Bull., 52, No. 4, pp. 601-614.

Youssef N, Adham S, Celebi M, Malilay J (1992) Cairo, Egypt, Earthquake of October 12. 1992, EERI Newsletter, Vol. 26, No.12, December.

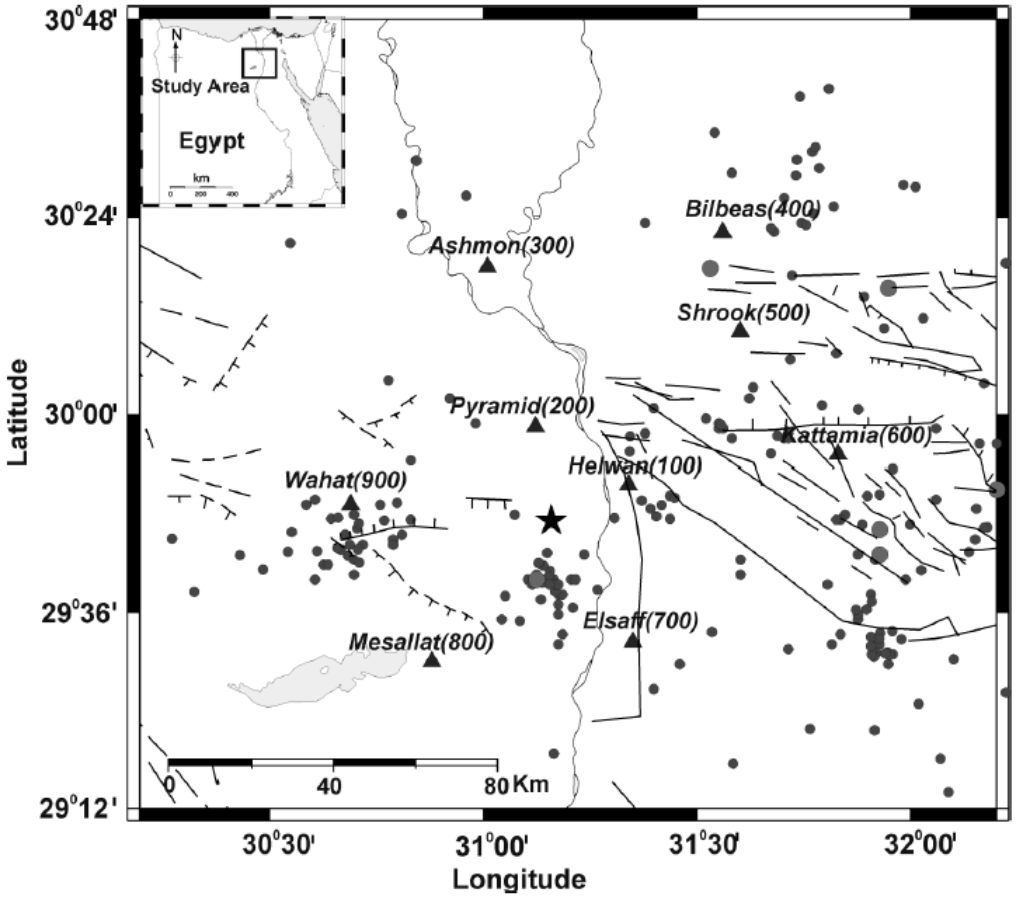

Fig.1. Seismotectonic map of Cairo region, the small circles show the earthquakes M=2-3, the large circles show the earthquakes M=3-4, the star indicates the largest earthquake at 12th October 1992 (M=5.9), the triangles show the GPS stations with their names and numbers.

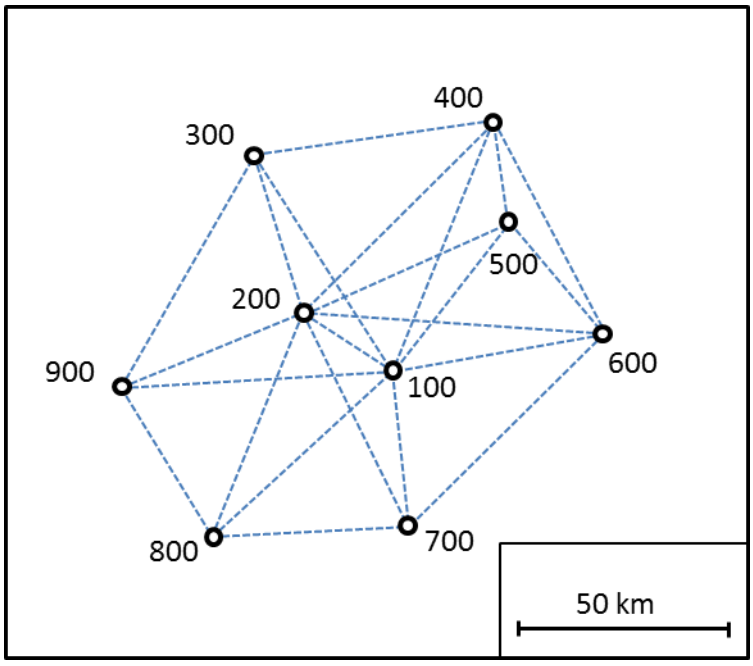

Fig. 2. The sketch of Cairo Network and the selected baselines

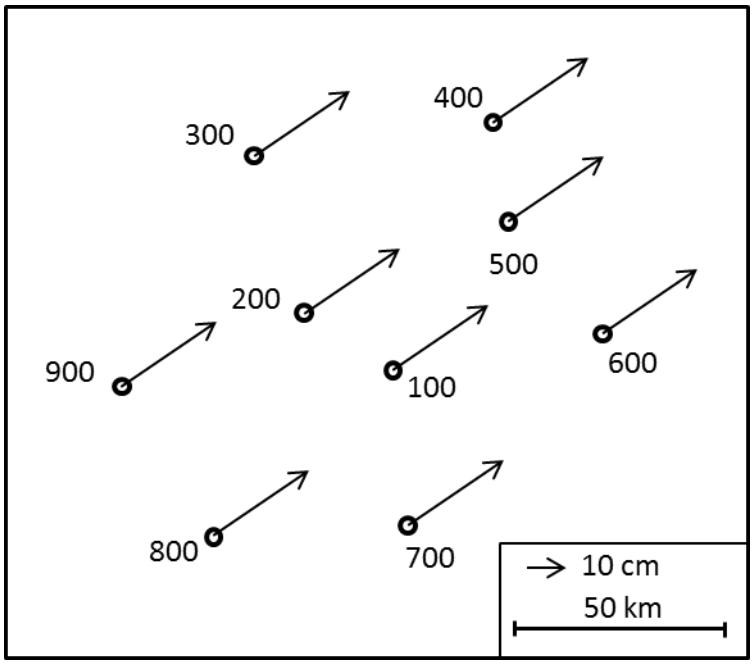

Fig. 3. The estimated horizontal plate motions for ten years.

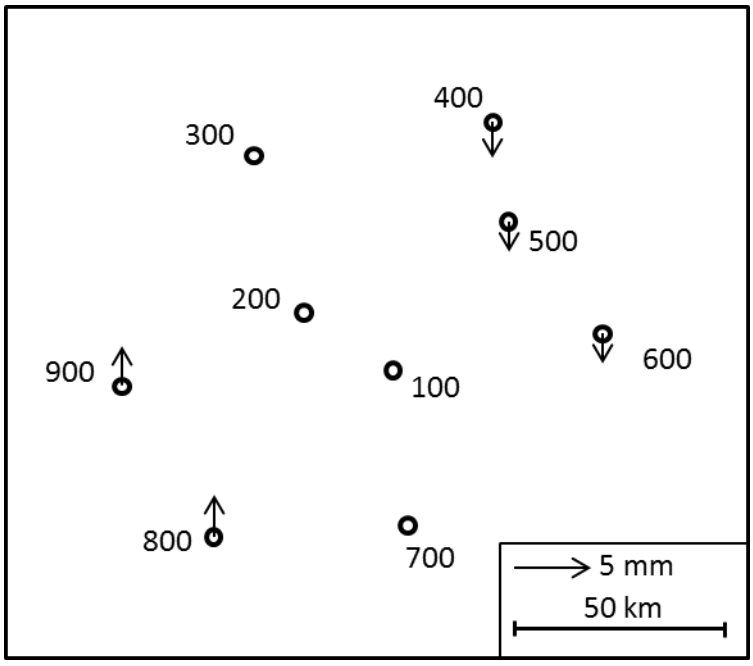

Fig. 4. Estimated vertical motions as the impact of residual plate motions

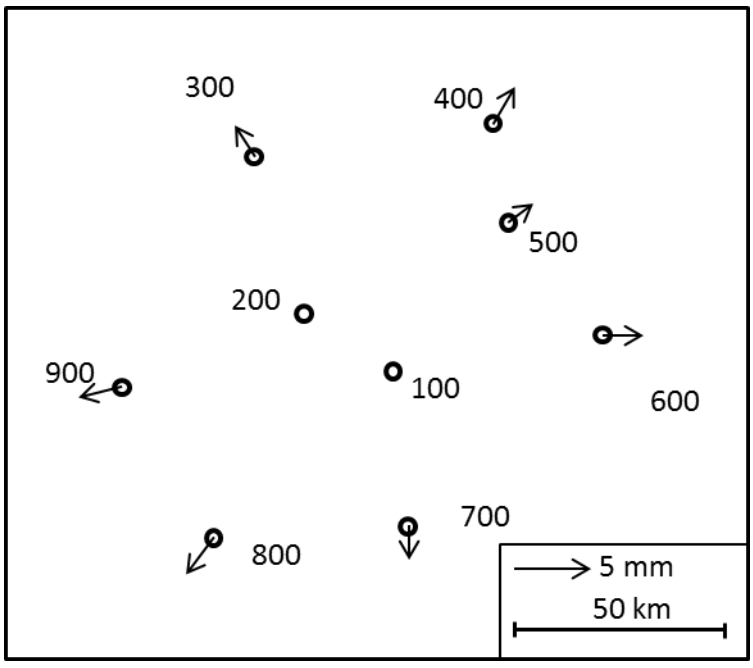

Fig. 5. Estimated horizontal motions as the impact of 0.05 ppm scale bias

Table 1. Simulated motion of the network using ITRF2000 (D&A) model (m)

	initial epoch	10 years plate motion			*simulated epoch*
Stations	*X* *Y* *Z*	*ΔX*	*ΔY*	*ΔZ*	*X* *Y* *Z*
100	4728141 2879661 3157147	-0.1995	0.1661	0.1473	4728140.8005 2879661.1661 3157147.1473
200	4733789 2858114 3168117	-0.1990	0.1663	0.1474	4733788.8010 2858114.1663 3168117.1474
300	4723885 2839244 3199346	-0.1993	0.1658	0.1658	4723884.8007 2839244.1658 3199346.1471
400	4692946 2882752 3205908	-0.2011	0.1647	0.1463	4692945.7989 2882752.1647 3205908.1463
500	4700632 2891947 3186688	-0.2008	0.1650	0.1465	4700631.7992 2891947.1650 3186688.1465
600	4700712 2917884 3163657	-0.2011	0.1651	0.1466	4700711.7989 2917884.1651 3163657.1466
700	4742146 2889985 3126746	-0.1990	0.1667	0.1477	4742145.8010 2889985.1667 3126746.1477
800	4767118 2851785 3123591	-0.1975	0.1676	0.1484	4767117.8025 2851785.1676 3123591.1484
900	4762265 2826732 3153862	-0.1975	0.1674	0.1482	4762264.8025 2826732.1674 3153862.1482
mean stand. dev.		-0.1994 0.0015	0.1661 0.0011	0.1473 0.0008	

Table (2). Transformation of ITRF2000 (D&A) motions,
the translations are in m, the rotations are in arcsec

unknown	*global*		*shifted*	
t_x	0.0013	±0.0014	-0.1994	±0.0000
t_y	0.0007	±0.0019	0.1661	±0.0000
t_z	-0.0001	±0.0018	0.1473	±0.0000
R_x	-0.0005	±0.0002	-0.0005	±0.0002
R_y	0.0061	±0.0001	0.0061	±0.0001
R_z	-0.0075	±0.0001	-0.0075	±0.0001
sc	0.0001	±0.0001	0.0001	±0.0001

Table 3. Baseline changes using ITRF2000 (D&A) model (m)

Baselines	*length (km)*	10 years changes		
		ΔX	*ΔY*	*ΔZ*
400-500	23	0.0003	0.0003	0.0002
200-100	25	-0.0005	-0.0002	-0.0001
500-600	35	-0.0003	0.0001	0.0001
100-700	35	0.0005	0.0006	0.0004
200-300	38	-0.0003	-0.0005	-0.0003
900-800	40	0.0000	0.0002	0.0002
100-500	42	-0.0013	-0.0011	-0.0008
200-900	45	0.0015	0.0011	0.0008
800-700	46	-0.0015	-0.0009	-0.0007
100-600	47	-0.0016	-0.0010	-0.0007
200-500	51	-0.0018	-0.0013	-0.0009
200-700	53	0.0000	0.0004	0.0003
300-400	54	-0.0018	-0.0011	-0.0008
400-600	55	0.0000	0.0004	0.0003
200-800	56	0.0015	0.0013	0.0010
100-800	59	0.0020	0.0015	0.0011
100-300	59	0.0002	-0.0003	-0.0002
100-400	60	-0.0016	-0.0014	-0.0010
300-900	61	0.0018	0.0016	0.0011
200-400	61	-0.0021	-0.0016	-0.0011
600-700	62	0.0021	0.0016	0.0011
100-900	63	0.0020	0.0013	0.0009
200-600	68	-0.0021	-0.0012	-0.0008
mean	49	-0.0001	0.0000	0.0000
stand. dev.	12	0.0014	0.0011	0.0008

Table 4. Coordinate changes (m) after the baseline adjustment using only translational constraints (the effect of plate motion)

stations	*north*	*east*	*up*
100	0.0000	0.0001	-0.0000
200	-0.0001	-0.0000	0.0005
300	-0.0001	-0.0003	-0.0001
400	0.0002	-0.0003	-0.0023
500	0.0002	-0.0002	-0.0019
600	0.0004	0.0001	-0.0020
700	0.0000	0.0003	0.0008
800	-0.0002	0.0003	0.0027
900	-0.0004	0.0002	0.0025
mean	0.0000	0.0000	0.0000
stand. dev.	0.0002	0.0002	0.0018

Table 5. Transformations of the adjusted network, the translations are in m, the rotations are in arcsec (translational constraints, the effect of plate motion)

unknown	*Global*		*Shifted*	
t_x	0.1981	±0.0014	-0.0000	±0.0000
t_y	-0.1654	±0.0019	-0.0000	±0.0000
t_z	-0.1474	±0.0018	-0.0000	±0.0000
R_x	-0.0005	±0.0002	-0.0005	±0.0002
R_y	0.0061	±0.0001	0.0061	±0.0001
R_z	-0.0075	±0.0001	-0.0075	±0.0001
sc	0.0001	±0.0001	0.0001	±0.0001

Table 6. Baseline changes (m) caused by scale bias

Baselines	*length*	0.05 ppm		
	(km)	*ΔX*	*ΔY*	*ΔZ*
400-500	23	0.0004	0.0005	-0.0010
200-100	25	-0.0003	0.0011	-0.0005
500-600	35	0.0000	0.0013	-0.0012
100-700	35	0.0007	0.0005	-0.0015
200-300	38	-0.0005	-0.0009	0.0016
900-800	40	0.0002	0.0013	-0.0015
100-500	42	-0.0014	0.0006	0.0015
200-900	45	0.0014	-0.0016	-0.0007
800-700	46	-0.0012	0.0019	0.0002
100-600	47	-0.0014	0.0019	0.0003
200-500	51	-0.0017	0.0017	0.0009
200-700	53	0.0004	0.0016	-0.0021
300-400	54	-0.0015	0.0022	0.0003
400-600	55	0.0004	0.0018	-0.0021
200-800	56	0.0017	-0.0003	-0.0022
100-800	59	0.0019	-0.0014	-0.0017
100-300	59	-0.0002	-0.0020	0.0021
100-400	60	-0.0018	0.0002	0.0024
300-900	61	0.0019	-0.0006	-0.0023
200-400	61	-0.0020	0.0012	0.0019
600-700	62	0.0021	-0.0014	-0.0018
100-900	63	0.0017	-0.0026	-0.0002
200-600	68	-0.0017	0.0030	-0.0002
mean	49	0.0000	0.0004	-0.0003
stand. dev.	12	0.0014	0.0015	0.0015

Table 7. Coordinate changes (m) after the baseline adjustment
using only translational constraints
(the effect of 0.05 ppm scale bias)

stations	*north*	*east*	*up*
100	-0.0004	0.0004	0.0000
200	0.0002	-0.0007	0.0000
300	0.0020	-0.0013	0.0000
400	0.0024	0.0014	0.0000
500	0.0012	0.0016	0.0000
600	-0.0001	0.0027	0.0000
700	-0.0022	0.0004	0.0000
800	-0.0024	-0.0018	0.0000
900	-0.0007	-0.0028	0.0000
mean	0.0000	0.0000	0.0000
stand. dev.	0.0017	0.0018	0.0000

Table 8. Transformation of adjusted network,
the translations are in m, the rotations are in arcsec
(translational constraints, the effect of 0.05 ppm scale bias)

unknown	*global*		*shifted*	
t_x	-0.2372	±0.0016	-0.0000	±0.0000
t_y	-0.1423	±0.0021	0.0000	±0.0000
t_z	-0.1574	±0.0020	-0.0000	±0.0000
R_x	-0.0000	±0.0001	-0.0000	±0.0002
R_y	-0.0000	±0.0001	-0.0000	±0.0001
R_z	0.0000	±0.0001	0.0000	±0.0001
sc	0.0499	±0.0002	0.0499	±0.0001

Table 9. Coordinate changes (m) after the baseline adjustment
using only translational constraints
(the effect of plate motion and 0.05 ppm scale bias)

stations	*north*	*east*	*up*
100	-0.0004	0.0004	-0.0000
200	0.0000	-0.0007	0.0005
300	0.0019	-0.0016	-0.0001
400	0.0026	0.0011	-0.0023
500	0.0014	0.0014	-0.0019
600	0.0003	0.0028	-0.0020
700	-0.0022	0.0007	0.0008
800	-0.0026	-0.0015	0.0027
900	-0.0010	-0.0026	0.0025
mean	0.0000	0.0000	0.0000
stand. dev.	0.0018	0.0017	0.0018

Table 10. Transformation of the adjusted network, the translations are in m, the rotations are in arcsec (translational constraints, the effect of plate motion and 0.05 ppm scale bias)

unknown	*global*		*shifted*	
t_x	-0.0405	±0.0021	-0.0000	±0.0000
t_y	-0.3131	±0.0027	0.0000	±0.0000
t_z	-0.3056	±0.0026	-0.0000	±0.0000
R_x	-0.0004	±0.0001	-0.0004	±0.0001
R_y	0.0061	±0.0001	0.0061	±0.0001
R_z	-0.0076	±0.0001	-0.0076	±0.0001
sc	0.0507	±0.0003	0.0507	±0.0003

Table 11. Baseline changes (m) caused by plate motion, 0.05 ppm scale bias and $N(0,1)$ mm noise

Baselines	*length*	combined		
	(km)	ΔX	ΔY	ΔZ
400-500	23	0.0008	0.0004	-0.0014
200-100	25	-0.0009	-0.0013	-0.0010
500-600	35	-0.0006	0.0013	-0.0011
100-700	35	0.0020	0.0007	-0.0029
200-300	38	-0.0005	-0.0012	0.0042
900-800	40	0.0001	0.0015	-0.0016
100-500	42	-0.0045	0.0010	0.0012
200-900	45	0.0015	-0.0001	0.0008
800-700	46	-0.0022	0.0018	0.0004
100-600	47	-0.0038	0.0012	0.0001
200-500	51	-0.0029	0.0010	-0.0014
200-700	53	-0.0011	0.0032	-0.0037
300-400	54	-0.0046	0.0008	-0.0002
400-600	55	0.0025	0.0024	-0.0014
200-800	56	0.0020	0.0014	-0.0013
100-800	59	0.0047	0.0008	0.0007
100-300	59	-0.0003	-0.0033	0.0008
100-400	60	-0.0038	-0.0016	0.0012
300-900	61	0.0038	0.0002	0.0008
200-400	61	-0.0043	-0.0001	0.0003
600-700	62	0.0028	0.0000	-0.0014
100-900	63	0.0048	-0.0013	0.0011
200-600	68	-0.0037	0.0028	-0.0001
mean	49	-0.0003	0.0005	-0.0002
stand. dev.	12	0.0030	0.0015	0.0016

Table 12. Coordinate changes (m) after the baseline adjustment using only translational constraints (the effect of plate motion, 0.05 ppm scale bias and $N(0,1)$ mm noise)

stations	*north*	*east*	*up*
100	-0.0003	0.0001	-0.0001
200	-0.0001	-0.0011	0.0007
300	0.0018	-0.0018	0.0001
400	0.0028	0.0014	-0.0028
500	0.0011	0.0018	-0.0020
600	0.0002	0.0029	-0.0014
700	-0.0029	0.0011	0.0004
800	-0.0025	-0.0014	0.0025
900	-0.0002	-0.0029	0.0029
mean	0.0000	0.0000	0.0000
stand. dev.	0.0018	0.0019	0.0019

Table 13. Transformations of the adjusted network the translations are in m, the rotations are in arcsec (translational constraints, the effect of plate motion, 0.05 ppm scale bias and $N(0,1)$ mm noise)

unknown	*global*		*shifted*	
t_x	-0.0532	±0.0192	-0.0000	±0.0001
t_y	-0.3294	±0.0256	-0.0000	±0.0001
t_z	-0.3135	±0.0247	-0.0000	±0.0001
R_x	0.0002	±0.0008	0.0002	±0.0001
R_y	0.0063	±0.0007	0.0063	±0.0001
R_z	-0.0075	±0.0008	-0.0075	±0.0001
sc	0.0539	±0.0027	0.0539	±0.0027

Table 14. Coordinate changes (m) and the estimated parameters (integrated model, effect of plate motion, 0.05 ppm scale bias and $N(0,1)$ mm noise

stations	*north*	*east*	*up*
100	0.0001	-0.0003	-0.0001
200	-0.0002	-0.0004	0.0002
300	-0.0002	-0.0003	0.0001
400	0.0002	0.0001	-0.0005
500	-0.0004	0.0002	-0.0001
600	0.0001	-0.0001	0.0007
700	-0.0005	0.0005	-0.0004
800	0.0002	0.0003	-0.0002
900	0.0007	0.0000	0.0003
mean	0.0000	0.0000	0.0000
stand. dev.	0.0004	0.0003	0.0004
R_x	0.0002	±0.0012	arcsec
R_y	0.0063	±0.0012	arcsec
R_z	-0.0076	±0.0012	arcsec
sc	0.0539	±0.0012	ppm

Table 15. Coordinate changes (m) and the estimated parameters (integrated model, effect of plate motion, 0.05 ppm scale bias and $N(0,1)$ mm noise, the single movements of stations 400, 500 and 600 are allowed)

stations	*north*	*east*	*up*
100	0.0001	-0.0003	0.0001
200	-0.0002	-0.0003	0.0002
300	-0.0002	-0.0002	-0.0002
400	**-0.0168**	**-0.0244**	**-0.0005**
500	**-0.0173**	**-0.0243**	**0.0000**
600	**-0.0168**	**-0.0246**	**0.0010**
700	-0.0006	0.0005	-0.0001
800	0.0002	0.0003	-0.0001
900	0.0007	0.0000	0.0001
mean*	0.0000	0.0000	0.0000
stand. dev.*	0.0004	0.0003	0.0002
R_x	0.0010	±0.0014	arcsec
R_y	0.0057	±0.0015	arcsec
R_z	-0.0088	±0.0017	arcsec
sc	0.0533	±0.0017	ppm

*without stations 400, 500 and 600